

Pushing the envelope: microinjection of *Minute virus of mice* into *Xenopus* oocytes causes damage to the nuclear envelope

Sarah Cohen and Nelly Panté

Correspondence
Nelly Panté
pante@zoology.ubc.ca

Department of Zoology, University of British Columbia, 6270 University Boulevard, Vancouver, BC, Canada V6T 1Z4

Parvoviruses are small DNA viruses that replicate in the nucleus of their host cells. It has been largely assumed that parvoviruses enter the nucleus through the nuclear pore complex (NPC). However, the details of this mechanism remain undefined. To study this problem, the parvovirus *Minute virus of mice* (MVM) was microinjected into the cytoplasm of *Xenopus* oocytes and a transmission electron microscope was used to visualize the effect of the virus on the host cell. It was found that MVM caused damage to the nuclear envelope (NE) in a time- and concentration-dependent manner. Damage was predominantly to the outer nuclear membrane and was often near the NPCs. However, microinjection experiments in which the NPCs were blocked showed that NE damage induced by MVM was independent of the NPC. To address the question of whether this effect of MVM is specific to the NE, purified organelles were incubated with MVM. Visualization by electron microscopy revealed that MVM did not affect all intracellular membranes. These data represent a novel form of virus-induced damage to host cell nuclear structure and suggest that MVM is imported into the nucleus using a unique mechanism that is independent of the NPC, and involves disruption of the NE and import through the resulting breaks.

Received 12 February 2005

Accepted 31 August 2005

INTRODUCTION

In order to replicate, many viruses must be able to enter the nucleus of their host cell. In the nucleus, the virus gains access to the cellular machinery for DNA replication, transcription and RNA processing. However, in addition to providing numerous benefits, entry to the nucleus poses a serious challenge for the virus. The nuclear envelope (NE) acts as a barrier between the cytoplasm and the nucleus, and transport of cargo into and out of the nucleus is tightly regulated by the cell. The NE consists of a double membrane, the inner nuclear membrane (INM) and the outer nuclear membrane (ONM). Embedded in the NE are the nuclear pore complexes (NPCs), large protein assemblies that regulate bidirectional macromolecular transport between the nucleus and the cytoplasm. Nuclear import of molecules between 9 and 39 nm in diameter (Panté & Kann, 2002) is highly selective, energy- and temperature-dependent, and requires signals on the cargo molecule and soluble transport receptors (reviewed by Fahrenkrog & Aebi, 2003; Fried & Kutay, 2003; Pemberton & Paschal, 2005). These receptors recognize the signal and carry the cargo through the NPC using a mechanism that is still unresolved, although several models have been proposed (reviewed by Becskei & Mattaj, 2005).

Viruses have evolved various strategies to gain entry to the nucleus. Most viruses enter through the NPCs, using specific

nuclear localization sequences (NLSs) in viral proteins that bind cellular nuclear transport receptors (importins or karyopherins). The viral protein–importin complex then docks at the cytoplasmic face of the NPC and is actively transported into the nucleus; in contrast, many retroviruses enter the nucleus only during mitosis, when the membrane barrier is temporarily absent (reviewed by Smith & Helenius, 2004; Whittaker *et al.*, 2000).

At approximately 26 nm in diameter, parvoviruses are among the smallest known viruses (Llamas-Saiz *et al.*, 1997; Tsao *et al.*, 1991). They are non-enveloped, with a single-stranded DNA genome of ~5 kb, and replicate in the nucleus of actively dividing cells during S phase (Muzyczka & Berns, 2001). Thus, transport into the host nucleus is necessary for productive infection. Entry of parvoviruses into the host cell has been studied, as have the early stages of virus trafficking (reviewed by Vihinen-Ranta *et al.*, 2004). Parvoviruses enter cells by receptor-mediated endocytosis. Several cell surface receptors have been identified for different parvoviruses and the uptake process appears to involve clathrin-coated vesicles (Bartlett *et al.*, 2000; Parker & Parrish, 2000). Despite these important advances in the parvovirus cellular entry pathway, very little is known about nuclear import of parvoviruses.

Immunofluorescence experiments either with fluorescently labelled virus or with antibodies against capsid proteins have

shown that the capsid enters the nucleus (Bartlett *et al.*, 2000; Seisenberger *et al.*, 2001; Vihinen-Ranta *et al.*, 2000). However, these studies lack the resolution necessary to visualize whether the virus particles entering the nucleus are partially disassembled. For example, it is possible that the capsid disassembles in the cytosol and that the fluorescent signal seen in the nucleus comes from fluorescent-labelled capsid proteins. Nevertheless, it has been largely assumed that the intact parvovirus enters the nucleus through the NPC. In contrast, a single study has suggested that for adeno-associated virus (AAV), nuclear entry occurs independently of the NPC (Hansen *et al.*, 2001). This suggestion is based on experiments in which AAV was incubated with purified nuclei in the absence of factors necessary for NPC-mediated import and in the presence of wheat germ agglutinin (WGA), a lectin that is known to bind to the NPC and inhibit nuclear import (Dabauvalle *et al.*, 1988; Finlay *et al.*, 1987). WGA did not inhibit nuclear import of AAV, suggesting that the NPC is not necessary for virus entry. However, an alternative mechanism has not been defined.

Despite limited knowledge of the mechanisms of parvovirus nuclear import, some work has been done on nuclear import of parvoviral capsid proteins. Parvoviral capsids consist of 60 copies of three proteins, VP1 (83 kDa), VP2 (64 kDa) and VP3 (60 kDa) (Muzyczka & Berns, 2001). VP2 is the major structural protein composing ~90% of the capsid. VP1 and VP2 are expressed from overlapping reading frames and thus the two proteins are identical in amino acid sequence except for the first 142 residues of VP1 (Weichert *et al.*, 1998). Several potential NLSs are located in the N-terminal sequence of VP1 and one of these is able to mediate the nuclear import of a heterologous protein (Vihinen-Ranta *et al.*, 1997). Thus, it has been suggested that VP1 may mediate nuclear import of the parvovirus. However, the N-terminal sequence of VP1 is enclosed within the capsid (Cotmore *et al.*, 1999) and therefore it is not clear how it would mediate nuclear import of the virus. Similarly, a sequence directing nuclear import of VP2 has been identified (Lombardo *et al.*, 2000; Pillet *et al.*, 2003). Because newly synthesized capsid proteins must reach the nucleus to permit assembly of new virus particles, the NLSs on VP1 and VP2 may be involved only in the nuclear import of newly synthesized capsid proteins and not in the nuclear import of intact capsids. Thus, additional work is required to determine whether these sequences serve as signals directing not only nuclear import of the capsid proteins, but nuclear import of the intact capsids.

To investigate the mechanism of parvovirus nuclear transport, the parvovirus *Minute virus of mice* (MVM) was microinjected into the cytoplasm of *Xenopus* oocytes and its nuclear uptake was followed by electron microscopy (EM). Our data indicate that MVM causes small breaks in the NE that are able to support nuclear import of protein in oocytes where the NPCs were blocked with WGA. A mechanism of parvovirus nuclear entry is proposed that involves disruption of the NE and import through the resulting breaks.

METHODS

Cells, virus and oocytes. Adherent HeLa cells (ATCC) were maintained at 5% CO₂ and 37 °C in Dulbecco's modified Eagle's medium (HyClone) supplemented with 10% fetal bovine serum (FBS) and penicillin/streptomycin. MVM was propagated in mouse fibroblast LA9 cells (Littlefield, 1964) that were grown in suspension in an environment of 5% CO₂ and 37 °C in Joklik modified minimum essential medium Eagle (Sigma) supplemented with 5% FBS and 25 mM HEPES (both cells and MVM were kindly provided by C. Astell, British Columbia Genome Sciences Center, Vancouver, Canada). After effective infection of LA9 cells, MVM was purified through two rounds of CsCl gradient centrifugation according to the original protocol of Tattersall *et al.* (1976) with the modification described by Williams *et al.* (2004), which consists of replacing the sucrose gradient by a second CsCl gradient. Purified MVM was titred by plaque assay as described by Tattersall *et al.* (1976).

Mature (stage VI) oocytes were surgically removed from narcotized *Xenopus laevis* as described by Panté (2006). Oocytes were washed three times with modified Barth's saline buffer [MBS: 88 mM NaCl, 1 mM KCl, 0.82 mM MgSO₄, 0.33 mM Ca(NO₃)₂, 0.41 mM CaCl₂, 10 mM HEPES, pH 7.5] and defolliculated by treatment with collagenase (5 mg ml⁻¹; Sigma) in calcium-free MBS for 1 h. Defolliculated oocytes were washed three times with MBS and stored in MBS.

Oocyte microinjection. Micropipettes (Microcaps; Drummond) were heated and pulled using a micropipette puller (Inject-Matic). Microinjection of *Xenopus* oocytes was performed as described by Panté (2006) using an oocyte microinjector (Inject-Matic). Oocytes were injected with about 100 nl purified MVM in the cytoplasm at the transitional zone between the animal and vegetal hemispheres. As control experiments, oocytes were mock-injected with 100 nl PBS.

For time-dependence experiments, oocytes were microinjected with purified MVM at a cellular concentration of 9.8×10^4 p.f.u. ml⁻¹ and then incubated at room temperature in MBS for 30 min, 1 h or 2 h. For concentration-dependence experiments, oocytes were microinjected with purified MVM at a cellular concentration of 9.8×10^1 , 9.8×10^3 or 9.8×10^4 p.f.u. ml⁻¹ and then incubated at room temperature in MBS for 1 h.

For inhibition of nuclear import through the NPC, oocytes were cytoplasmically microinjected with 50 nl WGA (20 mg ml⁻¹; Sigma) and incubated at room temperature for 6 h. After this incubation period, oocytes were microinjected with purified MVM at a cellular concentration of 9.8×10^4 p.f.u. ml⁻¹ and then incubated at room temperature in MBS for 2 h. Inhibition of nuclear import by WGA was confirmed in control oocytes that were microinjected with WGA, incubated as above and then microinjected with an import-competent substrate instead of MVM. This substrate was BSA cross-linked with synthetic *Simian virus 40* large T antigen NLS peptide (CGGGPKKKRKVED) and conjugated to colloidal gold (BSA-NLSg). The BSA-NLS was custom made by Sigma Genosys. Both colloidal gold particles (diameter ~8 nm) and NLS-BSAg were prepared as described by Panté (2006).

Preparation of injected oocytes for EM. After microinjection and incubation at room temperature for the indicated time, oocytes were prepared for embedding and thin-section EM following the protocol of Panté (2006). Briefly, oocytes were first fixed overnight at 4 °C with 2% glutaraldehyde in MBS. The following day, oocytes were washed with MBS and their animal hemispheres were dissected and fixed with 2% glutaraldehyde in low-salt buffer (LSB: 1 mM KCl, 0.5 mM MgCl₂, 10 mM HEPES, pH 7.5) for 1 h at room temperature. Dissected oocytes were washed with LSB, embedded in 2%

low-melting agarose and post-fixed with 1% OsO₄. Fixed oocytes were sequentially dehydrated in ethanol and embedded in Epon 812 (Fluka) as described by Panté (2006).

Thin sections (50 nm) through the NE were cut on a Leica Ultracut Ultramicrotome (Leica Microsystems) using a diamond knife (Diatome). Sections were placed on phalloidin/carbon-coated copper EM grids and stained with 2% uranyl acetate for 30 min and 2% lead citrate for 5 min. Micrographs were digitally recorded with a Hitachi-7600 transmission electron microscope.

Organelle isolation and assay. Rat liver nuclei were isolated as previously described (Gerace *et al.*, 1978). Approximately 8×10^6 rat liver nuclei were incubated for 2 h at room temperature in LSB with MVM at a ratio of 1 p.f.u. per nucleus. After incubation, nuclei were centrifuged at 16 000 g for 5 min. The resulting pellet was fixed and prepared for thin-section EM as described above.

Mitochondria were purified from HeLa cells using a kit from Sigma. Briefly, cells were homogenized in extraction buffer (10 mM HEPES, 200 mM mannitol, 70 mM sucrose, 1 mM EGTA, pH 7.5) by 25 strokes in a 3 ml homogenizer, to achieve ~80% lysis. Homogenization was followed by low- (600 g) and high-speed (11 000 g) centrifugation at 4°C. The pellet from the high-speed centrifugation contained mitochondria, which were then stored in storage buffer (10 mM HEPES, 250 mM sucrose, 1 mM ATP, 0.08 mM ADP, 5 mM sodium succinate, 2 mM K₂HPO₄, 1 mM DTT, pH 7.5).

Mitochondria from approximately 7.2×10^6 cells were incubated for 2 h at room temperature in storage buffer with MVM at a ratio of 1 p.f.u. per cell. After incubation, mitochondria were pelleted and prepared for EM as described above.

RESULTS

MVM damages the NE of *Xenopus* oocytes

In order to address the question of parvovirus nuclear import, MVM was microinjected into the cytoplasm of *Xenopus* oocytes. *Xenopus* oocytes are widely used to study NPC structure and function. Microinjection of *Xenopus* oocytes with import substrates followed by EM is an excellent system for studying nuclear import *in vivo* because oocytes have a high NPC density and yield structurally well preserved NPCs, so that import of substrates (including viral capsids) can be followed through single NPCs. This system has been used to characterize the nuclear import of various cellular substrates, as well as viruses such as *Hepatitis B virus* (Görlich *et al.*, 1996; Panté & Aebi, 1996; Panté & Kann, 2002; Rabe *et al.*, 2003; Rollenhagen *et al.*, 2003).

In contrast to oocytes microinjected with other import substrates that have shown the substrate crossing the NPC (Görlich *et al.*, 1996; Panté & Aebi, 1996; Panté & Kann, 2002; Rabe *et al.*, 2003; Rollenhagen *et al.*, 2003), MVM was not seen in transit through NPCs. Instead, it was observed that at 1 h post-injection (p.i.), the virus caused small breaks (~100–200 nm) in the NE (Fig. 1). Damage was predominantly to the ONM and was often near the NPCs (Fig. 1b; breaks marked with *). MVM particles, identified by their round shape, diameter and dense appearance, appeared to be associated with the ONM and close to where the ONM was disrupted (Fig. 1b, breaks marked with **, and 1d, arrows). Occasionally, virus particles were observed between the ONM and INM, in close proximity to breaks in the ONM (Fig. 1c, arrows). Unusual membrane structures associated with the NE were also observed; for example, vesicles between the ONM and INM (Fig. 1e and Fig. 3d, arrows).

and 1d, arrows). Occasionally, virus particles were observed between the ONM and INM, in close proximity to breaks in the ONM (Fig. 1c, arrows). Unusual membrane structures associated with the NE were also observed; for example, vesicles between the ONM and INM (Fig. 1e and Fig. 3d, arrows).

NE damage induced by MVM is time-dependent

The effect of virus incubation time on the NE was further investigated and it was found that damage to the NE was time-dependent (Fig. 2). As early as 30 min p.i., small breaks of 119 ± 13 nm were observed in the ONM (Fig. 2b and e). These breaks occurred only in the ONM, not in the INM. In a region of approximately 1.5 µm, a mean of 2.0 ± 0.2 NE breaks was observed at 30 min p.i. At 1 h p.i., similar damage was observed; on average, the breaks occurred at the same frequency (2.0 ± 0.2 breaks per 1.5 µm region), but were slightly larger (139 ± 15 nm) than the breaks observed at 30 min. However, at 1 h p.i., large stretches of damage to the ONM, up to 400 nm long and spanning one or more NPC (Fig. 2c), were occasionally observed. At 2 h p.i., NE breaks were significantly larger (216 ± 29 nm) and more frequent (3.1 ± 0.2 breaks per 1.5 µm region) and were not restricted to the ONM. In approximately 50% of the breaks ($51 \pm 6\%$), both the INM and ONM were affected. In many cases, both the ONM and INM appeared to be completely obliterated, leaving behind only strange 'shadow pore' versions of NPCs (Fig. 2d, arrow).

In order to better quantify membrane damage, three oocytes were examined for each treatment. For each oocyte, micrographs of 10 regions of approximately 1.5 µm containing 5–15 NPCs were studied. For each region, the number of breaks was counted and the length of the breaks was measured. The total length of the breaks was divided by the length of the ONM to find the proportion of membrane damaged (Fig. 2f). At 30 min and 1 h p.i., approximately 15% of the ONM was damaged. At 2 h p.i., this proportion increased dramatically, more than doubling to almost 40% damage. In mock-injected samples, approximately 2% damage to the NE was observed. This is likely because junctions where the NE is continuous with the endoplasmic reticulum occasionally appear as breaks in thin-section EM. Breaks in mock-injected samples had a mean length of only 24 ± 7 nm, which is significantly smaller than the breaks observed in oocytes injected with MVM.

NE damage induced by MVM is concentration-dependent

In addition to being time-dependent, damage to the NE was also concentration-dependent (Fig. 3). Oocytes were injected with MVM at cellular concentrations of 9.8×10^1 , 9.8×10^3 or 9.8×10^4 p.f.u. ml⁻¹, incubated at room temperature for 1 h and prepared for EM. As illustrated in Fig. 3, it was found that damage increased with virus concentration. Membrane damage was quantified as described

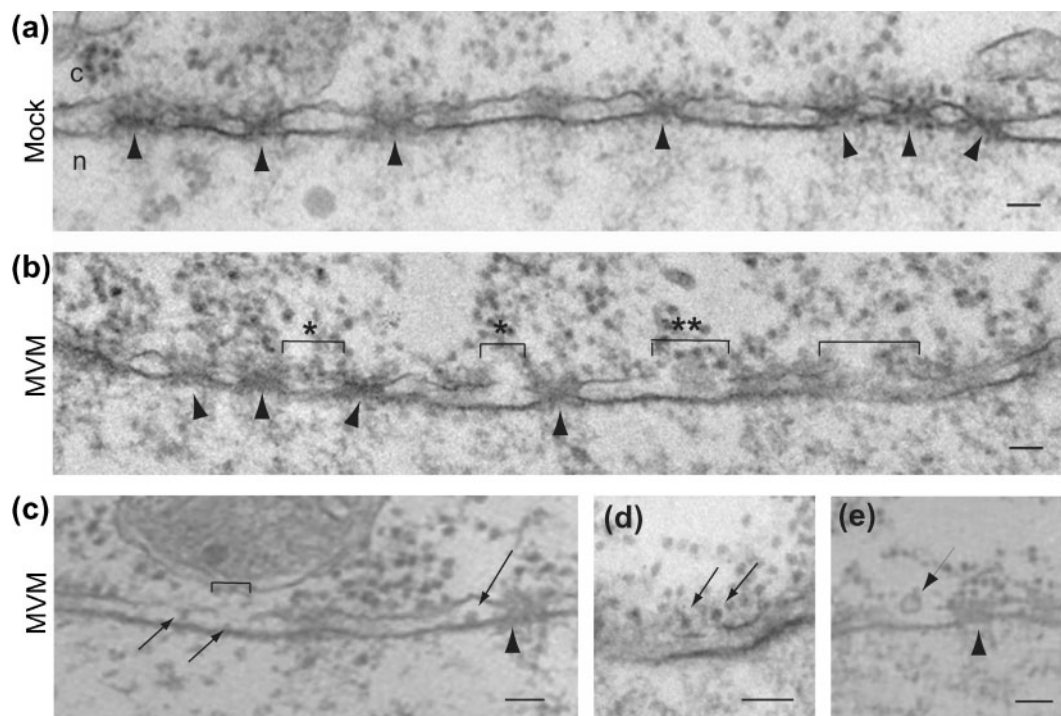


Fig. 1. MVM damages the ONM of *Xenopus* oocytes. Views of NE cross-sections with adjacent cytoplasm (c) and nucleus (n) from *Xenopus* oocytes that have been mock-injected with PBS (a) or injected with MVM (b–e). After injection, oocytes were incubated for 1 h at room temperature and processed for embedding and thin-section EM. Arrowheads, NPCs. Brackets indicate breaks in the NE caused by MVM. Often some of these breaks were found close to NPCs (indicated by *). Virus capsids were shown associated with the ONM (d, arrows), close to the ONM breaks (b, indicated by **) and in the perinuclear space (c, arrows). Sometimes small vesicles were found close to the ONM breaks (e, arrow). Bars, 100 nm.

above for time-dependence experiments: the mean break length, frequency of breaks, and proportion of NE damaged in mock injections and oocytes injected with different concentrations of MVM are represented in Fig. 3(e and f). Because of the 1 h incubation period, damage was usually restricted to the ONM for the different virus concentrations. As shown in the bar graph in Fig. 3(e), the length and frequency of breaks increased with the intracellular virus concentration. Although the mean break length was similar in oocytes injected with 9.8×10^1 and 9.8×10^3 p.f.u. ml⁻¹, the frequency of breaks increased in oocytes injected with 9.8×10^3 p.f.u. ml⁻¹. Similarly, the proportion of NE damaged increased with virus concentration.

NE damage induced by MVM is independent of the NPC

To determine whether the NPC is necessary for nuclear import of MVM, MVM was microinjected into oocytes after blocking the NPCs with WGA. Oocytes were pre-injected with WGA (20 mg ml⁻¹), incubated for 6 h, microinjected with MVM, incubated for 2 h and prepared for thin-section EM. Import-competent NLS-BSAg was microinjected into the cytoplasm of control oocytes to confirm inhibition of nuclear import by WGA (Fig. 4a). When BSA-NLSg was microinjected into *Xenopus* oocytes in the absence of WGA,

gold particles were observed passing through the NPC and in the nucleus (data not shown). However, in oocytes pre-injected with WGA, BSA-NLSg was observed near the NPCs in range of the NPC filaments (Fig. 4a, arrows), but was not observed passing through the NPCs or in the nucleus. These observations are in agreement with similar results reported by Panté & Aebi (1996) and effectively demonstrate that the NPCs were blocked by WGA.

Having confirmed inhibition of nuclear import through the NPC, MVM was microinjected into oocytes pre-injected with WGA. In these oocytes, damage to the NE with the same characteristics described above for time-dependence experiments at 2 h p.i. was observed: NE breaks of approximately 200 nm affecting both the INM and ONM (Fig. 4b). Breaks in oocytes microinjected with WGA and MVM were 236 ± 24 nm long, compared with 212 ± 32 nm in oocytes microinjected with MVM alone, and occurred at a frequency of 2.4 ± 0.2 breaks per 1.5 μ m region, compared with 3.0 ± 0.2 breaks per region for MVM alone (Fig. 5a). The proportion of membrane damage was also very similar. In oocytes pre-injected with WGA, $38 \pm 3\%$ of the NE was damaged, compared with $39 \pm 4\%$ for those microinjected with MVM alone (Fig. 5b). Thus, MVM-induced damage to the NE seems to be independent of the NPC.

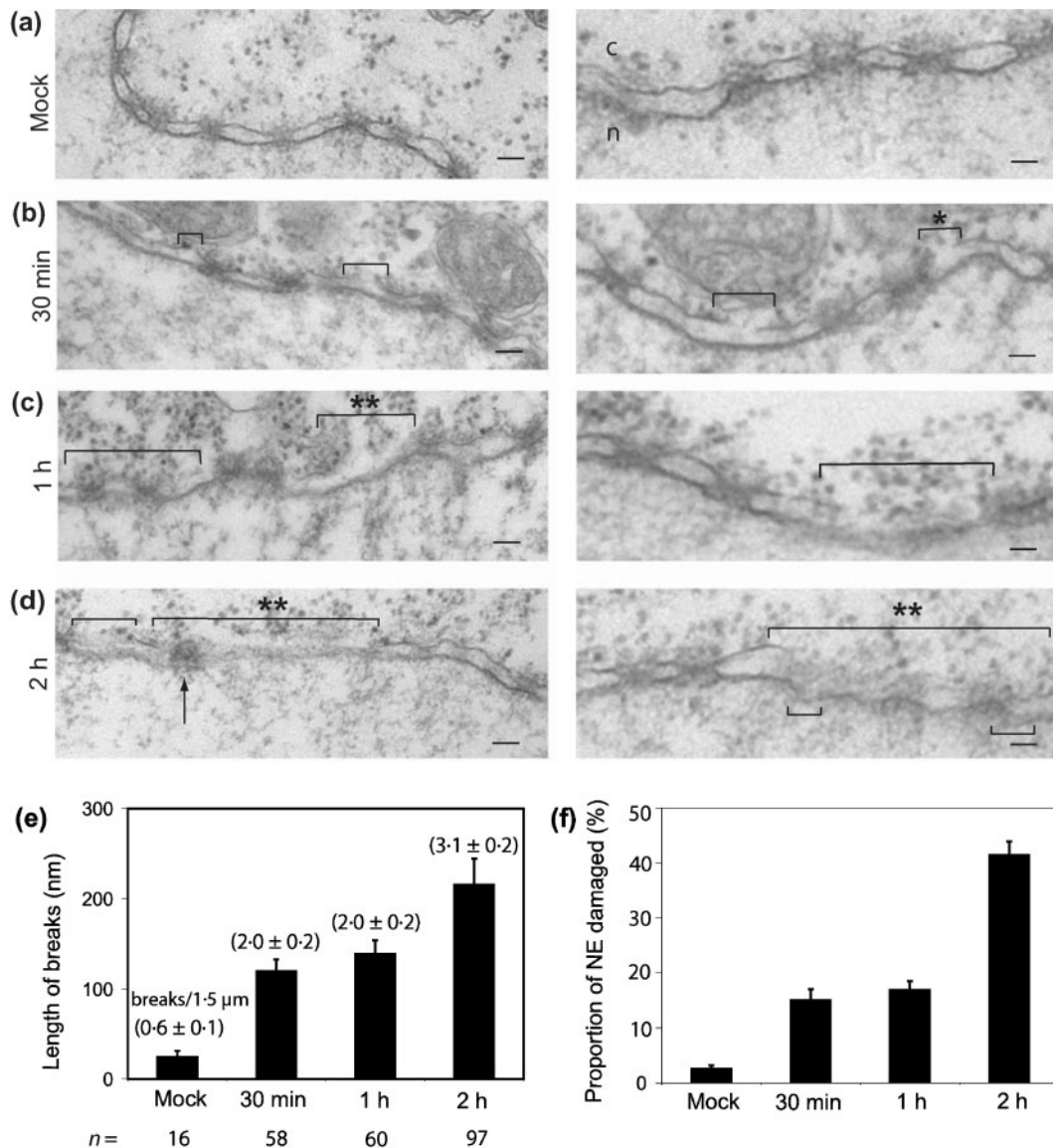


Fig. 2. NE damage induced by MVM is time-dependent. Views of NE cross-sections with adjacent cytoplasm (c) and nucleus (n) from *Xenopus* oocytes that have been mock-injected with PBS (a) or injected with MVM and processed for embedding and thin-section EM after 30 min (b), 1 h (c) and 2 h (d) incubation at room temperature. Whereas the mock-injected oocytes yielded intact nuclear membranes, the MVM-injected oocytes showed breaks (indicated by brackets) in the NE with dimensions that increased with incubation time. Often some of these breaks were close to NPCs (indicated by *). Virus particles associated with the NE are indicated by **. (a–d) Bars, 100 nm (left panels) and 200 nm (right panels). (e and f) Quantification of the NE damage induced by MVM after different incubation times. (e) Bar graph of the length of the ONM breaks measured from EM cross-sections of NE from experiments performed as indicated in (a–d). Numbers in parentheses indicate the mean and standard error of the number of breaks found in an NE region of 1.5 μ m. (f) Bar graph of the proportion of NE damage calculated as the length of the ONM breaks divided by the total length of the ONM from micrographs of experiments performed as indicated in (a–d). Each bar graph (e and f) shows the mean values and standard error measured for 30 micrographs obtained from three different oocytes examined for each condition, which yielded the number of breaks (*n*) as shown in (e).

It was then tested to see whether the NE breaks induced by MVM were able to support nuclear import of BSA-NLSg in oocytes that had been microinjected with WGA. In oocytes microinjected with WGA and BSA-NLSg, no gold was

observed in the nucleus (Fig. 4a); however, in oocytes injected with WGA, MVM and BSA-NLSg, BSA-NLSg particles were able to enter the nucleus through NE breaks induced by MVM (Fig. 4c, arrows). This shows that the

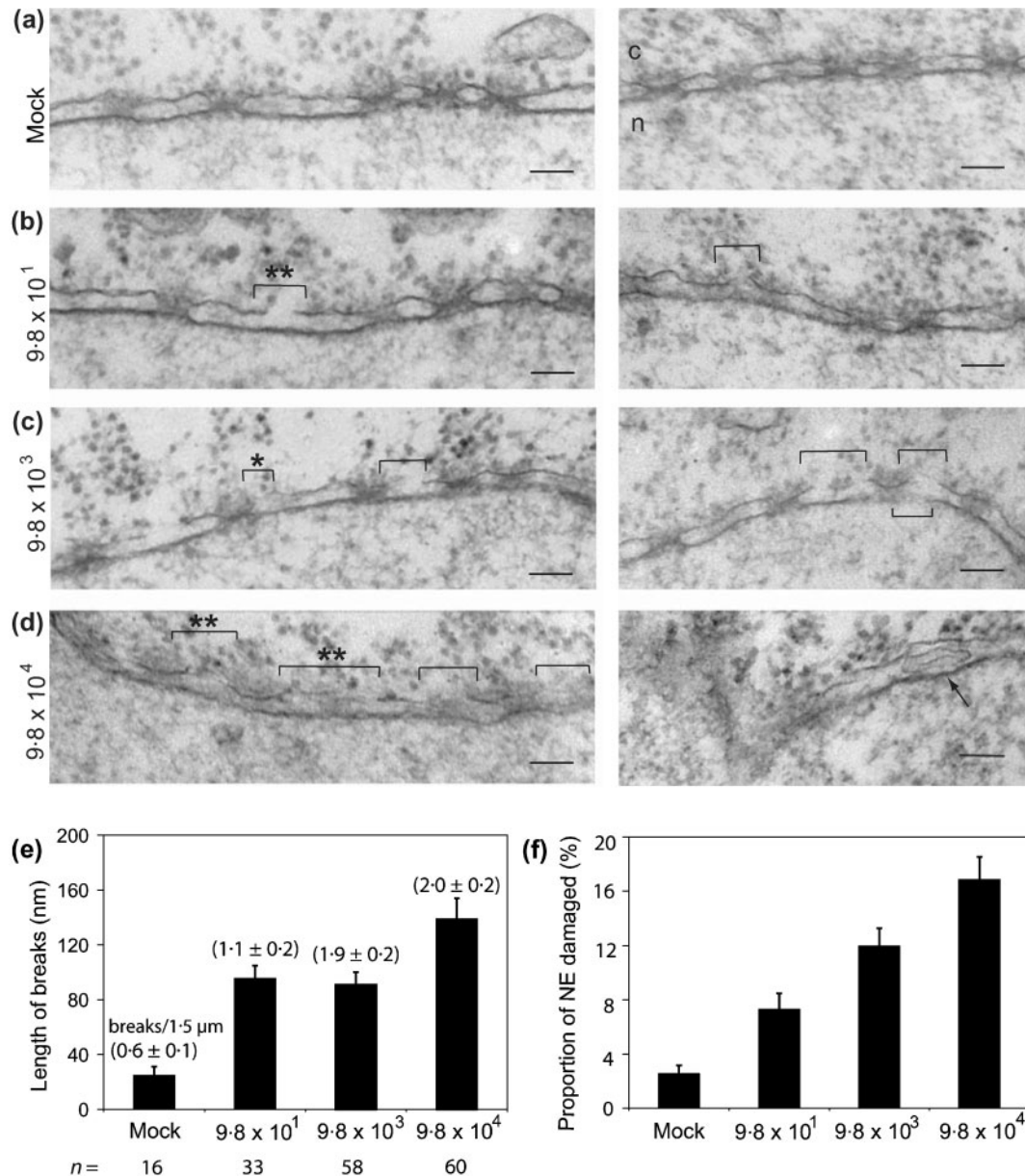


Fig. 3. NE damage induced by MVM is concentration-dependent. Views of NE cross-sections with adjacent cytoplasm (c) and nucleus (n) from *Xenopus* oocytes that have been mock-injected with PBS (a) or injected with different concentrations of MVM (b–d). All oocyte samples were incubated for 1 h at room temperature after injection and then processed for embedding and thin-section EM. The final intracellular concentration of MVM (p.f.u. ml⁻¹) is indicated on the left. Whereas mock-injected oocytes yielded intact nuclear membranes, the MVM-injected oocytes showed breaks (indicated by brackets) of the ONM with dimensions that increased with the intracellular concentration of MVM. Often some of these breaks were close to NPCs (indicated by *) and unusual vesicle structures were found in the perinuclear space for oocytes injected with high virus concentration (d, arrow). Virus particles associated with the NE are indicated by **. Bars (a–d), 100 nm. (e and f) Quantification of NE damage induced by MVM at different intracellular concentrations. (e) Bar graph of the length of the ONM breaks measured from EM cross-sections of NE from experiments performed as indicated in (a–d). Numbers in parentheses indicate the mean and standard error of the numbers of breaks found in an NE region of 1.5 μ m. (f) Bar graph of the proportion of NE damage calculated as the length of the ONM breaks divided by the total length of the ONM from micrographs of experiments performed as indicated in (a–d). Each bar graph (e and f) shows the mean values and standard error measured for 30 micrographs obtained from three different oocytes examined for each condition, which yielded the number of breaks (n) as shown in (e).

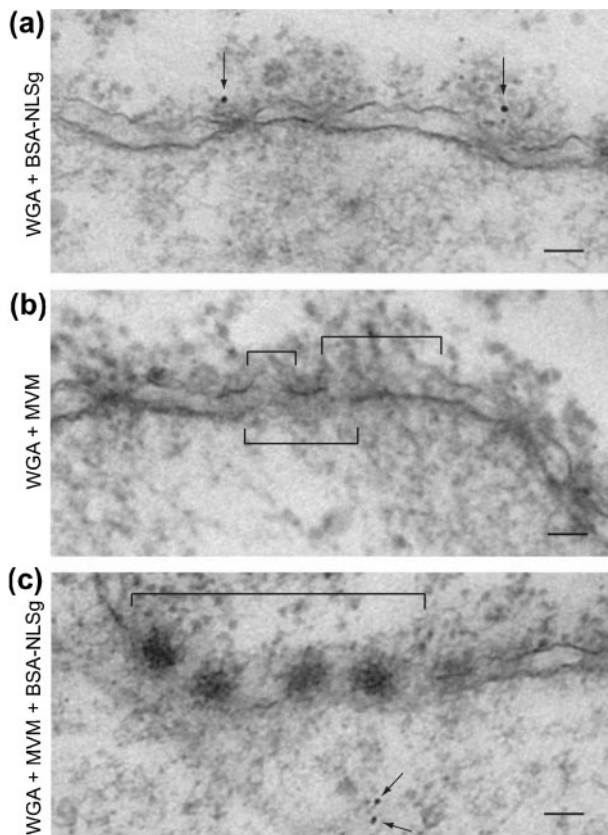


Fig. 4. NE damage induced by MVM is independent of the NPC. Views of NE cross-sections with adjacent cytoplasm (c) and nucleus (n) from *Xenopus* oocytes that have been injected with WGA (20 mg ml^{-1}), incubated at room temperature for 6 h, and then injected with BSA-NLSg (a), MVM (b) or MVM and BSA-NLSg (c). All oocyte samples were incubated for 2 h at room temperature after the second injection and then processed for embedding and thin-section EM. MVM-induced NE breaks in (b) and (c) are indicated by brackets. Arrows in (a) point to BSA-NLSg that is associated with the cytoplasmic face of NPCs, but did not enter the nucleus, indicating that nuclear import has been inhibited by WGA. Arrows in (c) point to BSA-NLSg that was able to enter the nucleus through the MVM-induced NE breaks. Bars, 100 nm.

damage to the NE caused by MVM does indeed facilitate nuclear import in an NPC-independent manner.

MVM does not induce damage in all intracellular membranes

Next, the question of whether MVM affects other intracellular membranes in addition to the NE was investigated. In *Xenopus* oocytes there are many mitochondria in the cytoplasm, which are structurally well preserved for EM. Damage to mitochondrial membranes in oocytes micro-injected with MVM was not observed; in fact, perfectly intact mitochondrial membranes were observed directly next to NE exhibiting severe damage (Fig. 6). However, to

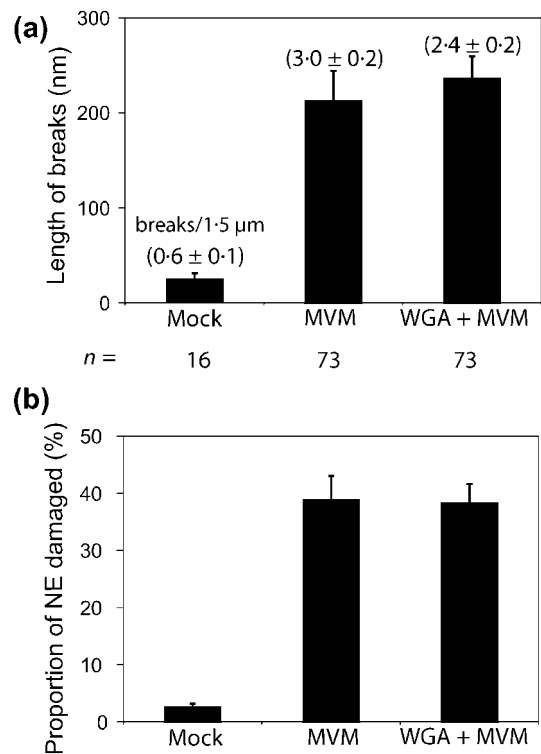


Fig. 5. Quantification of NE damage induced by MVM in the presence and absence of WGA. (a) Bar graph of the length of the ONM breaks measured from EM cross-sections of NE from experiments performed as indicated in Figs 2(d) and 4(b). Length of breaks induced by MVM in the presence of WGA (right bar) is compared to that in oocytes injected only with MVM (middle bar). Numbers in parentheses indicate the mean and standard error of the numbers of breaks found in an NE region of $1.5 \mu\text{m}$. (b) Bar graph of the proportion of NE damage calculated as the length of ONM breaks divided by the total length of the ONM from EMs of experiments performed as indicated in Figs 2(d) and 4(b). Proportion of NE damage induced by MVM in the presence of WGA (right bar) is compared to that in oocytes injected only with MVM (middle bar). Each bar graph shows the mean values and standard error measured for 30 micrographs obtained from three different oocytes examined for each condition, which yielded the number of breaks (n) as shown in (a).

further investigate this question, the effects of MVM on purified rat liver nuclei and on mitochondria purified from HeLa cells were examined.

Purified organelles were incubated with MVM for 2 h at room temperature and visualized by EM. Rat liver nuclei incubated with MVM exhibited distinct breaks in the ONM, similar in appearance to those seen in the NE of micro-injected oocytes (Fig. 7a). Virus particles were often seen associated with these breaks (Fig. 7a, *). In contrast, no effect was observed on mitochondrial membranes (Fig. 7b). Out of 50 mitochondria examined, none exhibited breaks in

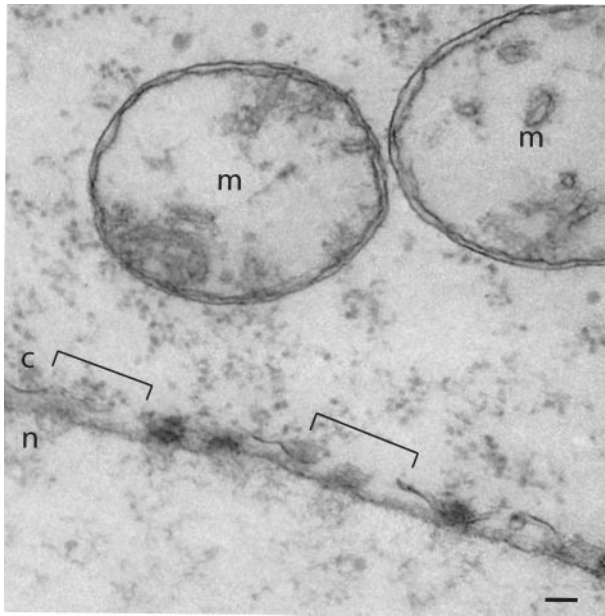


Fig. 6. MVM does not induce damage in all intracellular membranes of *Xenopus* oocytes. View of NE cross-section with adjacent cytoplasm (c) and nucleus (n) from a *Xenopus* oocyte that has been injected with MVM. Breaks in the ONM are apparent (brackets). However, the membranes of adjacent mitochondria (m) are entirely intact. Bar, 100 nm.

the outer or inner mitochondrial membranes. Thus, MVM does not cause damage to all intracellular membranes.

DISCUSSION

It has been largely assumed that parvovirus enters the nucleus through the NPC. In order to characterize this mechanism, MVM was microinjected into the cytoplasm of *Xenopus* oocytes and EM was used to visualize its nuclear import. In contrast to the current theory of parvovirus nuclear import, it was found that MVM injection caused breaks in the NE. These breaks were predominantly in the ONM and represent a novel form of virus-induced damage to host cell nuclear structure. Often virus particles were observed between the ONM and INM, in close proximity to these breaks, suggesting that MVM is imported into the nucleus by a unique mechanism that involves disruption of the NE and passing through the resulting breaks.

Traditionally, crossing the NPC has been considered the only way for nuclear import substrates to enter the nucleus. Evidence has shown that several viruses that replicate in the nucleus also use the NPC to gain access to the nucleus (reviewed by Izaurralde *et al.*, 1999; Smith & Helenius, 2004; Whittaker *et al.*, 2000). However, our data show that MVM is an exception. Two possible ways to enter an intact nucleus from the cytoplasm without crossing the NPC can be envisioned. The first is by passing through the ONM and INM using a budding mechanism similar to pinocytosis.

Such a pathway has been observed in nuclear export of herpesviruses (Granzow *et al.*, 2001), but has not been observed as a means of nuclear import of any virus or any other import substrate. In the case of herpesviruses, after assembly in the nucleus, the capsids bud through the INM and acquire an envelope. In this process, the INM is left intact and enveloped viruses are seen in the perinuclear space. This does not seem to be the case for parvoviruses, since clear breaks in the ONM of MVM-injected oocytes were found and enveloped MVM particles were not observed in the perinuclear space.

The second possible mechanism for nuclear import that does not involve the NPC is disruption of the NE and entering the nucleus through the breaks. This is the mechanism that we favour for MVM. Ruptures of the NE to allow nuclear import have also been reported for the human immunodeficiency virus (HIV) protein R (Vpr) (de Noronha *et al.*, 2001). Vpr can induce transient herniations in the NE that burst, creating breaks in the NE (de Noronha *et al.*, 2001); it is thought that the pre-integration complex of HIV is then imported into the nucleus through these breaks (Segura-Totten & Wilson, 2001). How Vpr induces herniations is not well understood, but it is thought that after Vpr enters the nucleus through the NPC it weakens the NE at a few sites (Segura-Totten & Wilson, 2001). Thus, it is likely that NE damage starts at the INM and not at the ONM as for MVM.

Our results have revealed interesting characteristics of the distinct mechanism used by MVM to enter the nucleus. The NE damage induced by MVM seems to be independent of the NPC, since breaks are still observed *in vivo* in oocytes microinjected with MVM in the presence of WGA. This is consistent with *in vitro* studies showing that WGA does not inhibit nuclear uptake of AAV in purified nuclei (Hansen *et al.*, 2001). That BSA-NLSg gained entry to the nucleus in oocytes where the NPCs were blocked when MVM was co-injected demonstrates that NE breaks induced by MVM facilitate nuclear import in an NPC-independent manner. Our data reinforce the conclusion that parvoviruses do not require the NPC for nuclear import, but rather use a mode of virus entry to the nucleus that is different to that used by any other group of viruses known to date. An NPC-mediated mechanism of nuclear import for parvoviruses cannot be ruled out, but if this exists it is as one of multiple entry pathways. Since virus particles were never observed crossing the NPC in microinjected oocytes throughout the course of our EM work, we believe that entry through disruptions in the NE is the main nuclear import route of MVM.

In addition to being independent of the NPC, damage to the NE is also observed when MVM is incubated with purified rat liver nuclei, suggesting that cytosolic factors are not necessary for MVM to cause breaks in the NE. Moreover, MVM does not affect mitochondrial membranes, indicating that this mechanism is specific to certain intracellular membranes, including the NE and perhaps other similar

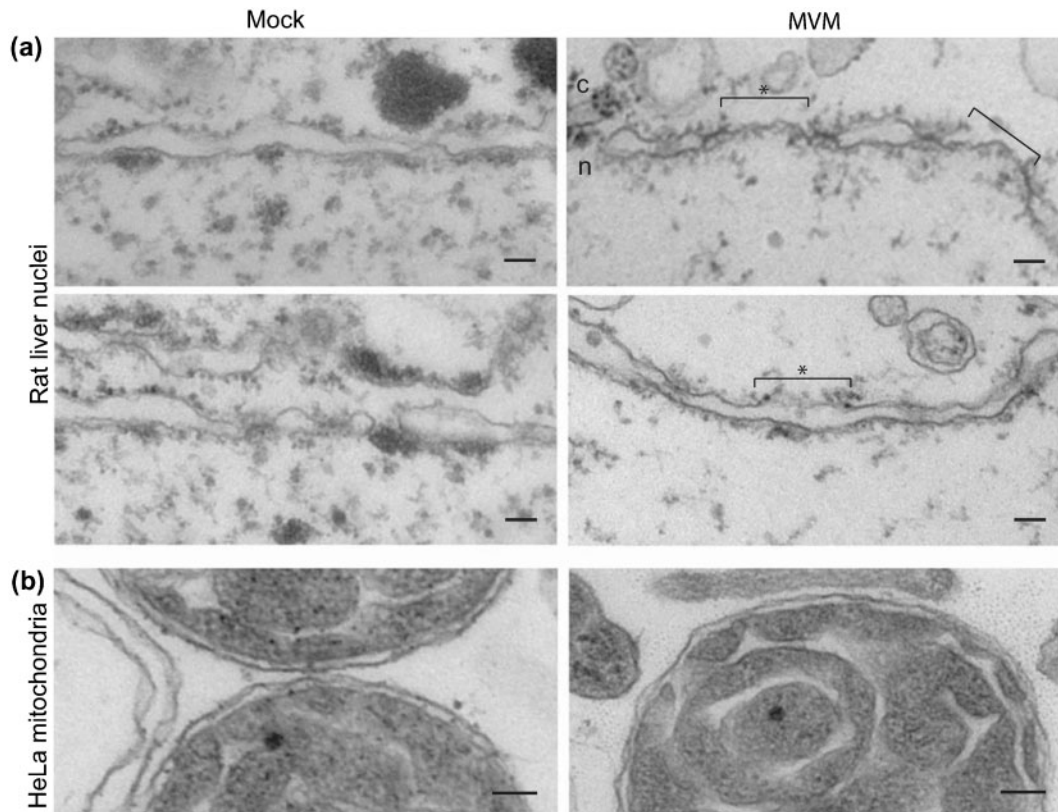


Fig. 7. MVM damages the membranes of nuclei, but not the membranes of mitochondria *in vitro*. Purified rat liver nuclei (a) or purified HeLa mitochondria (b) were incubated with PBS (left panels) or MVM (right panels) for 2 h at room temperature and then processed for embedding and thin-section EM. Whereas mock-incubated nuclei yielded intact NE, nuclei incubated with MVM showed breaks in the ONM (indicated by brackets) similar to those seen in *Xenopus* oocytes injected with MVM (Figs 1–3). Often virus particles were found associated with the ONM close to the breaks (indicated by *). Neither mock- nor MVM-incubated mitochondria showed breaks in the outer or inner membranes. Bars, 100 nm.

membranes. The basis of this specificity remains to be determined.

The unconventional MVM nuclear import route could be explained if MVM capsid proteins have membrane-lytic properties. Membrane-lytic peptides have been discovered in insects, amphibians and mammals, and may lyse prokaryotic or eukaryotic membranes (reviewed by Shai, 1999). Although the mechanism is not completely understood, it is thought that membrane-lytic peptides work either by inserting themselves into the membrane and creating hydrophilic pores or by interacting with phosphate head groups to disrupt membrane curvature, resulting in membrane lysis (Shai, 1999). It has also been shown that Vpr has membrane-lytic properties and can effectively permeabilize membranes (Coytaux *et al.*, 2003). It is possible that both MVM and Vpr cause NE breaks by directly lysing the NE, thereby facilitating nuclear entry. Thus, membrane-lytic peptides may play a previously unrecognized role in the nuclear import of diverse groups of viruses, including DNA and retroviruses.

ACKNOWLEDGEMENTS

We thank Dr Caroline Astell (British Columbia Genome Sciences Center) for providing the MVM and LA9 cells. This work was supported by grants from the Canada Foundation for Innovation (CFI), the Canadian Institute of Health Research (CIHR) and the Natural Sciences and Engineering Research Council of Canada (NSERC) to N. P.

REFERENCES

- Bartlett, J. S., Wilcher, R. & Samulski, R. J. (2000). Infectious entry pathway of adeno-associated virus and adeno-associated virus vectors. *J Virol* **74**, 2777–2785.
- Becskei, A. & Mattaj, I. W. (2005). Quantitative models of nuclear transport. *Curr Opin Cell Biol* **17**, 27–34.
- Coytaux, E., Coulaud, D., Le Cam, E., Danos, O. & Kichler, A. (2003). The cationic amphipathic alpha-helix of HIV-1 viral protein R (Vpr) binds to nucleic acids, permeabilizes membranes, and efficiently transfects cells. *J Biol Chem* **278**, 18110–18116.
- Cotmore, S. F., D'Abramo, A. M., Jr, Ticknor, C. M. & Tattersall, P. (1999). Controlled conformational transitions in the MVM virion

expose the VP1 N-terminus and viral genome without particle disassembly. *Virology* **254**, 169–181.

Dabauvalle, M. C., Schulz, B., Scheer, U. & Peters, R. (1988). Inhibition of nuclear accumulation of karyophilic proteins in living cells by microinjection of the lectin wheat germ agglutinin. *Exp Cell Res* **174**, 291–296.

de Noronha, C. M., Sherman, M. P., Lin, H. W., Cavois, M. V., Moir, R. D., Goldman, R. D. & Greene, W. C. (2001). Dynamic disruptions in nuclear envelope architecture and integrity induced by HIV-1 Vpr. *Science* **294**, 1105–1108.

Fahrenkrog, B. & Aebi, U. (2003). The nuclear pore complex: nucleocytoplasmic transport and beyond. *Nat Rev Mol Cell Biol* **4**, 757–766.

Finlay, D. R., Newmeyer, D. D., Price, T. M. & Forbes, D. J. (1987). Inhibition of in vitro nuclear transport by a lectin that binds to nuclear pores. *J Cell Biol* **104**, 189–200.

Fried, H. & Kutay, U. (2003). Nucleocytoplasmic transport: taking an inventory. *Cell Mol Life Sci* **60**, 1659–1688.

Gerace, L., Blum, A. & Blobel, G. (1978). Immunocytochemical localization of the major polypeptides of the nuclear pore complex-lamina fraction. Interphase and mitotic distribution. *J Cell Biol* **79**, 546–566.

Görlich, D., Panté, N., Kutay, U., Aebi, U. & Bischoff, F. R. (1996). Identification of different roles for RanGDP and RanGTP in nuclear protein import. *EMBO J* **15**, 5584–5594.

Granzow, H., Klupp, B. G., Fuchs, W., Veits, J., Osterrieder, N. & Mettenleiter, T. C. (2001). Egress of alphaherpesviruses: comparative ultrastructural study. *J Virol* **75**, 3675–3684.

Hansen, J., Qing, K. & Srivastava, A. (2001). Infection of purified nuclei by adeno-associated virus 2. *Mol Ther* **4**, 289–296.

Izaurralde, E., Kann, M., Panté, N., Sodeik, B. & Hohn, T. (1999). Viruses, microorganisms and scientists meet the nuclear pore. Lysin, VD, Switzerland, February 26–March 1, 1998. *EMBO J* **18**, 289–296.

Littlefield, J. W. (1964). The selection of hybrid mouse fibroblasts. *Cold Spring Harb Symp Quant Biol* **29**, 161–166.

Llomas-Saiz, A. L., Agbandje-McKenna, M., Wikoff, W. R., Bratton, J., Tattersall, P. & Rossmann, M. G. (1997). Structure determination of minute virus of mice. *Acta Crystallogr D Biol Crystallogr* **53**, 93–102.

Lombardo, E., Ramirez, J. C., Agbandje-McKenna, M. & Almendral, J. M. (2000). A beta-stranded motif drives capsid protein oligomers of the parvovirus minute virus of mice into the nucleus for viral assembly. *J Virol* **74**, 3804–3814.

Muzyczka, N. & Berns, K. I. (2001). *Parvoviridae*. In *Fields' Virology*, 4th edn, pp. 2327–2359. Edited by D. M. Knipe & P. M. Howley. Philadelphia: Lippincott Raven.

Panté, N. (2006). Use of intact *Xenopus* oocytes in nucleocytoplasmic transport studies. In *Methods in Molecular Biology*, vol. 322, *Xenopus Protocols: Cell Biology and Signal Transduction*, pp. 301–314. Edited by J. Liu. New Jersey: Humana Press. (in press)

Panté, N. & Aebi, U. (1996). Sequential binding of import ligands to distinct nucleopore regions during their nuclear import. *Science* **273**, 1729–1732.

Panté, N. & Kann, M. (2002). Nuclear pore complex is able to transport macromolecules with diameters of about 39 nm. *Mol Biol Cell* **13**, 425–434.

Parker, J. S. & Parrish, C. R. (2000). Cellular uptake and infection by canine parvovirus involves rapid dynamin-regulated clathrin-mediated endocytosis, followed by slower intracellular trafficking. *J Virol* **74**, 1919–1930.

Pemberton, L. F. & Paschal, B. M. (2005). Mechanisms of receptor-mediated nuclear import and nuclear export. *Traffic* **6**, 187–198.

Pillet, S., Annan, Z., Fichelson, S. & Morinet, F. (2003). Identification of a nonconventional motif necessary for the nuclear import of the human parvovirus B19 major capsid protein (VP2). *Virology* **306**, 25–32.

Rabe, B., Vlachou, A., Panté, N., Helenius, A. & Kann, M. (2003). Nuclear import of hepatitis B virus capsids and release of the viral genome. *Proc Natl Acad Sci U S A* **100**, 9849–9854.

Rollenhagen, C., Muhlhäusser, P., Kutay, U. & Panté, N. (2003). Importin β -depending nuclear import pathways: role of the adapter proteins in the docking and releasing steps. *Mol Biol Cell* **14**, 2104–2115.

Segura-Totten, M. & Wilson, K. L. (2001). Virology. HIV – breaking the rules for nuclear entry. *Science* **294**, 1016–1017.

Seisenberger, G., Ried, M. U., Endress, T., Buning, H., Hallek, M. & Brauchle, C. (2001). Real-time single-molecule imaging of the infection pathway of an adeno-associated virus. *Science* **294**, 1929–1932.

Shai, Y. (1999). Mechanism of the binding, insertion and destabilization of phospholipid bilayer membranes by α -helical antimicrobial and cell non-selective membrane-lytic peptides. *Biochim Biophys Acta* **1462**, 55–70.

Smith, A. E. & Helenius, A. (2004). How viruses enter animal cells. *Science* **304**, 237–242.

Tattersall, P., Cawte, P. J., Shatkin, A. J. & Ward, D. C. (1976). Three structural polypeptides coded for by minute virus of mice, a parvovirus. *J Virol* **20**, 273–289.

Tsao, J., Chapman, M. S., Agbandje, M. & 8 other authors (1991). The three-dimensional structure of canine parvovirus and its functional implications. *Science* **251**, 1456–1464.

Vihinen-Ranta, M., Kakkola, L., Kalela, A., Vilja, P. & Vuento, M. (1997). Characterization of a nuclear localization signal of canine parvovirus capsid proteins. *Eur J Biochem* **250**, 389–394.

Vihinen-Ranta, M., Yuan, W. & Parrish, C. R. (2000). Cytoplasmic trafficking of the canine parvovirus capsid and its role in infection and nuclear transport. *J Virol* **74**, 4853–4859.

Vihinen-Ranta, M., Suikkanen, S. & Parrish, C. R. (2004). Pathways of cell infection by parvoviruses and adeno-associated viruses. *J Virol* **78**, 6709–6714.

Weichert, W. S., Parker, J. S., Wahid, A. T., Chang, S. F., Meier, E. & Parrish, C. R. (1998). Assaying for structural variation in the parvovirus capsid and its role in infection. *Virology* **250**, 106–117.

Whittaker, G. R., Kann, M. & Helenius, A. (2000). Viral entry into the nucleus. *Annu Rev Cell Dev Biol* **16**, 627–651.

Williams, W. P., Tamburic, L. & Astell, C. R. (2004). Increased levels of B1 and B2 SINE transcripts in mouse fibroblast cells due to minute virus of mice infection. *Virology* **327**, 233–241.